Study of the electronic, magnetic and optical properties of lanthanum phosphide using first principle calculation

Student ID: 171328
Session: 2017-2018

Report submitted to the Department of Physics at
Jashore University of Science and Technology
in partial fulfillment of the requirements
for the degree of Bachelor of Science
with Honours in Physics

December 2022

Abstract

This study investigates the electronic, magnetic, and optical characteristics of LaP using the fully-potential linearized augmented plane wave technique (FP-LAPW) based on density functional theory (DFT). The rock-salt (RS) and zinc-blende (ZB) type structures are studied using the GGA and mBJ approaches. The calculated findings suggest that the indirect bandgap of LaP for ferromagnetic (FM) ZB type structures is 2.259 eV. LaP exhibits completely semiconducting behavior when studied for mBJ potential rather than GGA potential. According to the calculated optical properties such as dielectric function, refractive index, optical reflection, and optical conductivity, LaP is a promising candidate for optoelectronic applications.

Acknowledgements

Foremost, I praise and thank almighty Allah, the Lord of the worlds, the Most Merciful, the Guider of hearts, the Provider of sustenance, the Owner of life and death.

I would like to express my sincere gratitude to Dr. Mohammad Abdur Rashid who has provided unwavering support and guidence throughout the whole time. His immense knowledge and enthusiasm aided me in improving my problem solving capabilities.

My sincere thanks goes to all faculty members of Department of Physics for their encouragements and insightful comments which led me to prepare for my future career.

I would also like to thank my CCMP groupmates specially Nasrin Afroz who contributed to many discussion that helped me to shape this project.

My deepest appreciation belongs to my parents and my sister for their patience, understanding and supporting me spiritually throughout my life.

Contents

List of Figures

List of Tables

Study of the electronic, magnetic and optical properties of lanthanum phosphide using first principle calculation

Chapter 1

Introduction

The significance of rare-earth pnictides is growing faster as a result of their intricate structural, magnetic, and electronic properties [1]. They also exhibit intriguing semiconducting characteristics that are employed in a variety of real-world situations, including non-linear optics, electro-optical components, grinding alloys, composite lasers, and phosphor lasers [2]. Finding alternate sources of element recovery is necessary due to the element's continually increasing demand [3, 4]. Here, the first element of the lanthanide series coupled with the phosphorus combination, lanthanum-phosphide, is examined to see if it may be utilized for optoelectronic devices and to assess its potential in the future. Early research on the rare earth element GdP shows that it has semiconducting and spintronic characteristics [5]. Studying the electronic band structure and magnetic and optical characteristics of LaP would be fascinating because the majority of the rare earth pnictides investigated in earlier research show potential semiconducting activity [6, 7]. Most material qualities are governed by their electrical structure. Density Functional Theory (DFT) has been the standard computation technique in solid state physics over the last four decades [8]. The density distribution, $n(r)$, is the key variable in DFT, and it only depends on three coordinates, where N is the number of particles [9]. Densities, spin densities, ground state energies, and associated quantities like as lattice structures

and constants can be calculated without using parameters in DFT [10]. All complexity of the many-electron system are incorporated in the exchange-correlation (XC) functional in Kohn-Sham DFT [11]. Numerous solid-state features may be accurately predicted by using the traditional semilocal approximations to the XC functionals [12]. The full potential linearized augmented plane waves (FP-LAPW) approach, as used in the WIEK2k code, and the modified Becke Johnson (mBJ) method both achieve average accuracy even better than the GGA potential, which has been employed in this computation [13]. We calculated ZB and RS type structures both ferromagnetically and non-magnetically, and we found that the ferromagnetic computation of ZB type structures has more intriguing electrical and optical features.

Spintronics is the study of inherent spin and the magnetic moment of electron associated with them [14, 15]. Our LaP-based computing has a number of noteworthy properties, including semiconducting behavior for its ferromagnetic ordering. Rare-earth elements have become crucial parts of the periodic table because to their ubiquitous usage in spintronic applications [16]. Based on this computation, we can perform more intriguing future calculations that can broaden the spintronic fields.

This work is structured as follows: In Chapter 1, an introduction of quantum mechanical theory related to condensed matter physics will be offered to highlight the issue to be solved, namely, solving the many-body Schrödinger equation. In Chapter 2, DFT will be introduced as a theoretical method for tackling this problem. The exchange-correlation energy functional used in computations inside DFT will be described. In Chapter 3, we shall demonstrate the explanations and interpretations of our results. In Chapter 4, we will analyze our system's conclusion and probable consequences.

Chapter 2

Theoretical background

Science that studies how matter and light behave on an atomic and subatomic scale is known as quantum mechanics. It makes an effort to explain and describe the characteristics of molecules, atoms, and their building blocks, including electrons, protons, neutrons, and other less familiar particles like quarks and gluons. The quanta of electromagnetic energy, the uncertainty principle, the Pauli exclusion principle, and the wave theory of matter particles are the four main concepts of quantum mechanics that have been empirically demonstrated to be relevant to the behavior of nuclear particles at close ranges.

2.1 Schrödinger equation

In 1926, Erwin Schrödinger attempted to characterize so-called "matter waves" by using de Broglie's connections to describe hypothetical plane waves, which resulted in the most generic version of the famous equation named after him, the time-dependent Schrödinger equation. The Schrödinger equation is used in quantum physics to describe the motion and behavior of systems at the atomic and subatomic levels, and it employs a quantity known as the wave function, which in turn offers information on the system's behavior [17]. For example, if we square the wave

function, we get the probability distribution of the system, which tells us how likely it is that we will locate the system, say an electron, at some given position in space. Understanding how an electron behaves in a nucleus is based on the idea of energy conservation (Kinetic Energy + Potential Energy = Total Energy).

The Schrödinger equation must be solved to determine the values of wave functions. It can be written in full form as:

$$-\frac{\hbar^2}{2m}\frac{d^2\psi(x)}{dx^2} + U(x)\psi(x) = E\psi(x) \tag{2.1}$$

where m is the electron mass of the system, ψ is the wave function of the system, V is the potential energy of the system, E is the energy eigenvalue of the system.

This equation plays a central role in non-relativistic quantum mechanics. For N particles in three dimension the Hamiltonian is,

$$\hat{H} = \sum_{i}^{N} \frac{\hat{p_i^2}}{2m_i} + V(\vec{r}_1, \vec{r}_2, ..., \vec{r}_N, t) = -\frac{\hbar^2}{2}\sum_{i=1}^{N}\frac{1}{m_i} + V(\vec{r}_1, \vec{r}_2, ..., \vec{r}_N, t) \tag{2.2}$$

The corresponding Schrödinger equation can be written as,

$$i\hbar\frac{\partial}{\partial t}\Psi(\vec{r}_1, \vec{r}_2, ..., \vec{r}_N, t) = [-\frac{\hbar^2}{2}\sum_{i=1}^{N}\frac{1}{m_i}\vec{\nabla}^2 + V(\vec{r}_1, \vec{r}_2, ..., \vec{r}_N, t)]\Psi(\vec{r}_1, \vec{r}_2, ..., \vec{r}_N, t) \tag{2.3}$$

This is the time-dependent Schrödinger equation for many-body system. In this report, from now on only non-relativistic cases are considered. When the Hamiltonian has no time dependence, the time-independent Schrödinger equation is obtained. Not only is the time-independent Schrödinger equation simpler to handle, but understanding its solutions also gives key insight into how to manage the related time-dependent equation [18]. In this case the potential does not depend on time, like as $V(\vec{r}_1, \vec{r}_2, ..., \vec{r}_N, t)$. So, the Hamiltonian can be written as,

$$\hat{H} = -\frac{\hbar^2}{2m}\vec{\nabla}^2 + V(\vec{r}) \tag{2.4}$$

The strategy of variable separation yields the time-independent equation. The spa-

tial and temporal part of the wave function can be separated by this way,

$$\Psi(\vec{r}_1, \vec{r}_2, ..., \vec{r}_N, t) = \Psi(\vec{r}_1, \vec{r}_2, ..., \vec{r}_N)\tau(t) = \Psi(\vec{r}_1, \vec{r}_2, ..., \vec{r}_N)e^{-i\omega t} \tag{2.5}$$

So, the time-independent Schrödinger equation for many-body system can be written as,

$$E\Psi(\vec{r}_1, \vec{r}_2, ..., \vec{r}_N) = [-\frac{\hbar^2}{2}\sum_{i=1}^{N}\frac{1}{m_i}\nabla_i^2 + V(\vec{r}_1, \vec{r}_2, ..., \vec{r}_N)]\Psi(\vec{r}_1, \vec{r}_2, ..., \vec{r}_N) \tag{2.6}$$

The general eigenvalue equation becomes as,

$$E\Psi(\vec{r}_1, \vec{r}_2, ..., \vec{r}_N) = \hat{H}\Psi(\vec{r}_1, \vec{r}_2, ..., \vec{r}_N) \tag{2.7}$$

2.2 The wave function

In quantum physics, a wave function is a variable quantity that mathematically characterizes the wave properties of a particle. The value of a particle's wave function at a given place in space and time is connected to the probability of the particle being there at the moment. Wave function, denoted by the Greek symbol ψ, can be conceived of as an expression for the amplitude of the particle wave (or de Broglie wave), though amplitude has no physical importance for such waves [19]. However, the square of the wave function, ψ^2, has physical significance: the chance of discovering the particle described by a certain wave function at a given position and time is proportional to the value of ψ^2.

$$|\Psi(\vec{r}_1, \vec{r}_2, ..., \vec{r}_N)|^2 d\vec{r}_1, d\vec{r}_2, ..., d\vec{r}_N. \tag{2.8}$$

Equation (2.8) describes the probability that particles $1, 2, ..., N$ are located simultaneously in the corresponding volume element $d\vec{r}_1, d\vec{r}_2, ..., d\vec{r}_N$. If the positions of two particles are exchanged the overall probability density cannot depend on such

an exchange, i.e.

$$|\Psi(\vec{r}_1, \vec{r}_2, ..., \vec{r}_i, \vec{r}_j, ..., \vec{r}_N)|^2 = |\Psi(\vec{r}_1, \vec{r}_2, ..., \vec{r}_j, \vec{r}_i, ..., \vec{r}_N)|^2 \tag{2.9}$$

According to the probability interpretation, the integral of the probability density across all degrees of freedom in the system must equal to 1. This general requirement that a wave function must satisfy is called the normalization condition. Which is,

$$\int d\vec{r}_1 \int d\vec{r}_2 ... \int d\vec{r}_N |\Psi(\vec{r}_1, \vec{r}_2, ..., \vec{r}_N)|^2 = 1 \tag{2.10}$$

A physical acceptable wave function also requires this criterion. The wave function must be square-integrable and continuous across the whole spatial range. We may compute the expectation values of operators using a wave function, which also computes the expectation value of the appropriate observable for that wave function. For an observable $O(\vec{r}_1, \vec{r}_2, ..., \vec{r}_N)$ written as,

$$O = \langle O \rangle = \int d\vec{r}_1 \int d\vec{r}_2 ... \int d\vec{r}_N \Psi^*(\vec{r}_1, \vec{r}_2, ..., \vec{r}_N) \hat{O} \Psi(\vec{r}_1, \vec{r}_2, ..., \vec{r}_N) \tag{2.11}$$

2.3 The Born-Oppenheimer (BO) approximation

The electrons in a molecule are characterized using the BO approximation, which ignores the mobility of the atomic nuclei [20]. It is based on the fact that the mass of a molecule's nucleus is far bigger than the mass of an electron (more than 1000 times) [21]. The BO approximation assumes that the molecular wavefunction can be written in the form:

$$\psi_{total} = \psi_{electronic} \psi_{vibration} \psi_{rotation} \tag{2.12}$$

Therefore that the energies due to each type of motion are additive as,

$$E_{total} = E_{electronic} + E_{vibrational} + E_{rotational} \tag{2.13}$$

As a result, the many-body issue is reduced to the simpler problem of electrons moving in an external potential, such as that created by positively charged nuclei. The Schrödinger equation for this system is then

$$\hat{T}\psi + \hat{V}\psi = -i\hbar\frac{\partial\psi(x,t)}{\partial t} \tag{2.14}$$

where ψ is the many-electron wavefunction. In electronic structure calculations, this is the most important object to consider because it holds all of the information about the system of electrons. A probability amplitude for discovering a system of electrons in a given configuration is provided by this formula,

$$\psi = \psi(r_1, r_2, ...r_N) \tag{2.15}$$

where the r_n are the coordinates of the electrons. Again, spin is included in the coordinates r_n, so that $r = (x, y, z, \sigma)$ where σ is the spin coordinate and can take the values of ($\uparrow$ spin-up) or ($\downarrow$ spin-down). $\hat{T}$ is now the many-electron kinetic energy operator, acting on as

$$\hat{T}\psi = -\frac{1}{2}\bigtriangledown^2 r_n\psi \tag{2.16}$$

$\bigtriangledown^2 r_n$ is the many-electron potential operator, which acts on ψ as

$$\hat{V}\psi = -\frac{1}{2}\left(\sum_n \bigtriangledown^2_{n\neq m} \mid \frac{1}{r_n - m_n} \mid + v_{ext}(r_n)\right)\psi \tag{2.17}$$

where V_{ext} is the external potential in which the electrons are moving. For the system of electrons and nuclei is given by,

$$V_{ext}(r) = -\sum_{n,m} \mid \frac{Z_{l_m}}{r_n - R_{ln}} \mid \tag{2.18}$$

It results in the simple way for handling molecules. Based on the fact that nuclei are thousands of times heavier than electrons, the BO theory was developed. The mass of a proton is around 2000 times greater than that of an electron. The electrons can be thought of dynamically as particles that drag along with the nuclei without

needing a limited amount of time to relax, or adiabatically following the nuclear motion. The many-electron Schrödinger equation must be solved in accordance with the limitations of normalization and exchange anti-symmetry. As a result of normalization, any potential electron configuration is guaranteed to have the same probability to 1.

$$\psi(r_1, r_2, ..r_n, r_m, r_N) = -\psi(r_1, r_2, ..r_n, r_m, r_N) \tag{2.19}$$

Most of the time, we're solely concerned with the electronic system's ground state. This is the lowest-energy solution to the Schrödinger equation for time-independent many-electron systems.

$$\hat{T}\psi + \hat{V}\psi = E\psi \tag{2.20}$$

where E is the ground state energy of the system of electrons.

2.4 Hartee-Fock (HF) approximation

The HF approximation, which was recently developed, is a linear combination of atomic orbitals that approximates one-electron wave functions. The wave function is directly dependent on some conditions, such as: both it and its derivation must be continuous in order to be used in HF calculations. There is an endless possibility of identifying the particle at the site or places of discontinuity, which is impossible in the event of a discontinuity [22]. The wave function must meet certain conditions in order to be considered valid. Slater-type orbitals are atomic orbitals that have a certain shape and are used in nuclear physics [23]. HF theory is one of the most straightforward approximate theories for solving the many-body Hamiltonian that is currently accessible. In this calculation, a basic approximation to the many-body wavefunction is utilized, which asserts that the wavefunction is given by a single

Slater determinant of N spin-orbitals, which is the case in reality.

$$\psi = \frac{1}{\sqrt{N!}} \begin{vmatrix} \psi_1(x_1) & \psi_2(x_2) & \cdots & \psi_N(x_N) \\ \psi_1(x_1) & \psi_2(x_2) & \cdots & \psi_N(x_N) \\ \vdots & \vdots & \cdots & \vdots \\ \psi_1(x_1) & \psi_2(x_1) & \cdots & \psi_N(x_N) \end{vmatrix} \tag{2.21}$$

Here the variables x include the coordinates of space and spin. This simple ansatz for the wavefunction ψ captures much of the physics required for accurate solutions of the Hamiltonian. Most importantly, the wavefunction is antisymmetric with respect to an interchange of any two electron positions. This property is required by the Pauli exclusion principle, i.e

$$\psi(x_1, x_2, ..x_i, ...x_j, ...x_N) = -\psi(x_1, x_2, ..x_j, ...x_i, ...x_N) \tag{2.22}$$

We now introduce a Lagrange multiplier ϵ to impose the condition that the ψ are normalised, and minimise with respect to the ψ,

$$\frac{\partial}{\partial \psi} \left[\langle \hat{H} \rangle - \sum_j \xi_i \int \mid \psi_j \mid^2 dr \right] = 0 \tag{2.23}$$

An enormous simplification of the expressions for the orbitals ψ results which reduce to a set of one-electron equations of the form as,

$$-\frac{1}{2} \sum_n \bigtriangledown^2 \psi_i(r) + V_{ion}(r)\psi_i(r) + U(r)\psi_i(r) = \epsilon \psi_i(r) \tag{2.24}$$

where $U(r)$ is a non-local potential and the local ionic potential is denoted by $V_{ion}(r)$.

The full HF equations are given by,

$$\begin{aligned} \epsilon_i \psi_i(r) = \left(-\frac{1}{2} \bigtriangledown^2 + V_{ion}(r) \right) \psi(r) + \sum_j \int dr' \frac{\mid \psi_j(r') \mid^2}{\mid r - (r') \mid} \psi_i(r) \\ - \sum_j \delta_{\sigma_i \sigma_j} \int dr' \frac{\psi_j^*(r') \psi_i(r')}{\mid r - (r') \mid} \psi_j(r) \end{aligned} \tag{2.25}$$

The right-hand side of the equations is made up of four terms, as shown above. The kinetic energy contribution and the electron-ion potential are the first and second causes of the phenomenon. Lastly, the third component, often known as the Hartree term, is simply the electrostatic potential resulting from the charge distribution of N electrons. When $j = I$ the word involves an unphysical self-interaction of electrons, according to the way it is expressed. This term is terminated in the fourth term, which is the exchange term. In our case, the inclusion of the Pauli principle as well as the assumption of a determinantal form of the wavefunction result in the exchange term. The impact of exchange is that electrons with similar spins avoid colliding with one another.

2.4.1 Limitation of HF approach

Due to the assumption of a single-determinant form for the wavefunction, HF theory does not take into account electron correlation [24]. The electrons are subjected to an average non-local potential emanating from the other electrons, which might result in a poor description of the electronic structure when the potential is measured. HF theory is qualitatively true in many materials and compounds, but it is inadequately accurate to make precise quantitative predictions in many others, including metals. We will achieve a stable point in energy after many cycles of SCF if we utilize the HF approach and compute the energy (via SCF), which will be higher than the exact energy. Because we don't account for all electron interactions. This energy represents the upper bound of the molecule's ground state energy. We only investigate some electron correlations in HF. Other correlations, such as Coulombic correlations are ignored by this method since the two electron section of the Fock matrix only contains an average representation of the electron interactions. This is one of the main reasons why HF theory is not widely accepted among theorists [25]. It produces results that are quite close to the real thing. MP2, DFT and linked cluster methods are examples of higher theories. Among theorists, CCSD(T) is regarded as the gold standard. The main contribition to the correlation energy arises from the mean field approximation used in HF-method. That means one electron moves in the average field of the other ones, an approach which completely

neglects the intrinsic correlation of the electron movements.

2.5 Electron density

Emission spectra, or electron density, is a measure of how likely it is to detect an electron in a certain position around an object [26]. A further assertion of quantum physics is the existence of electrons as stationary waves, or clouds of negative charge that can be detected. According to this viewpoint, the electron density of a cloud is a quantity that tells us how much charge is;

$$\psi \Longleftrightarrow \psi^2 = \rho \tag{2.26}$$

there at each point in the cloud.

2.6 Thomas-Fermi model

One of the first tractable techniques for solving the many-electron problem was proposed by Thomas and Fermi. In this model the electron density $n(r)$ is the central variable rather than the wavefunction, and the total energy of a system is written as a functional $E^{TF}[n(r)]$ where square brackets are used to enclose the argument of the functional, which in this case is the density [27]. The Thomas-Fermi energy functional is composed of three terms,

$$E^{TF}[n(r)] = A_k \int n(r)^{5/3} dr + V_{ext}(r) dr + \frac{1}{2} \int \int \frac{n(r) n(r)^{'}}{\mid r - (r)^{'} \mid} dr dr^{'} \tag{2.27}$$

$$T^{TF}[n(r)] = \int t_0[n(r)] dr \tag{2.28}$$

For starters, we have the kinetic energy of a non-interacting gas of electrons. This form is obtained by integrating the kinetic energy density of a homogeneous electron gas $t_0[n(r)]$ which is obtained by summing all of the free-electron energy states

ϵ=$k^2/2$ up to the Fermi wave vector $K_F = [3\pi^2 n(r)]^{1/3}$.

$$t_0[n(r)] = \frac{2}{(2\pi)^3}\int \frac{k^2}{2} n_k dk = \frac{1}{(2\pi)^2}\int_0^{k_F} k^4 dk \tag{2.29}$$

n_k is the density of allowed states in reciprocal-space. This leads to the form given in with coefficient $A_k = (3\pi^2)^{2/3}$. The power-law dependence on the density can also be established on dimensional grounds. The second term is the classical electrostatic energy of attraction between the nuclei and the electrons, where $V_{ext}(r)$ is the static Coulomb potential arising from the nuclei [28].

Finally, the third term in represents the electron-electron interactions of the system, and in this case is approximated by the classical Coulomb repulsion between electrons, known as the Hartree energy.

$$v_{ext}(r) = -\sum_{j=1}^{M} \frac{Z_j}{\mid r - R_j \mid} \tag{2.30}$$

$$\delta([F(f)] - \mu C[f]) = 0 \tag{2.31}$$

The minimisation of a functional $F[f]$, subject to the constraint $C[f]$ leads to the following stationary condition, where ν is a constant known as the Lagrange multiplier. Minimising this leads to the solution of the corresponding Euler equation,

$$\frac{\delta([F(f)]}{\delta f} - \mu \frac{\delta([C(f)]}{\delta f} = 0 \tag{2.32}$$

Applying this method leads to the stationary condition,

$$\delta[E^{TF}[n(r)] - \mu(\int n(r)dr - N)] = 0 \tag{2.33}$$

which yields the so-called Thomas-Fermi equations. The Thomas-Fermi theory has several problems, the most significant of which is that it fails to predict atom bonding, preventing molecules and solids from forming. The most common source of

error is an incorrect approximation of kinetic energy,

$$\frac{5}{3}A_k n(r)^{2/3} + V_{ext}(r) + \int \frac{n(r)^{'}}{\mid r - (r)^{'} \mid} - \mu = 0 \tag{2.34}$$

Because kinetic energy makes up such a large part of a system's overall energy, even tiny mistakes can be deadly [29]. Another issue is the oversimplification of electron-electron interactions, which are dealt with in a traditional manner and hence fail to account for quantum phenomena such as the exchange interaction.

2.7 Hohenberg-Kohn theorems

Basically, any system that involves electrons moving under the influence of an external potential can benefit from the Hohenberg-Kohn theorem. Simply, they are as follows:

2.7.1 Theorem 1

The external potential $V_{ext}(r)$, and hence the total energy, is a unique functional of the electron density $n(r)$ [30].

The energy functional $E[n(r)]$ alluded to in the first Hohenberg-Kohn theorem can be written in terms of the external potential $V_{ext}(r)$ in the following way,

$$E[n(r)] = \int n(r)V_{ext}(r)dr + F[n(r)] \tag{2.35}$$

where $F[n(r)]$ is an unknown, but otherwise universal functional of the electron density $n(r)$ only. Correspondingly, a Hamiltonian for the system can be written such that the electron wavefunction ψ that minimises the expectation value gives the groundstate energy (assuming a non-degenerate groundstate),

$$E[n(r)] = \langle \psi \mid \hat{H} \mid \psi \rangle \tag{2.36}$$

The Hamiltonian can be written as,

$$\hat{H} = \hat{F} + \hat{V}_{ext} \tag{2.37}$$

where $\hat{F}$ is the electronic Hamiltonian consisting of a kinetic energy operator $\hat{T}$ and an interaction operator $\hat{V}_{ee}$,

$$\hat{F} = \hat{T} + \hat{V}_{ee} \tag{2.38}$$

The electron operator $\hat{F}$ is the same for all N-electron systems, so $\hat{H}$ is completely defined by the number of electrons N, and the external potential $V_{ext}(r)$ [31].

The proof of the first theorem is remarkably simple and proceeds by reduction. Let there be two different external potentials, $V_{ext,1}(r)$ and $V_{ext,2}(r)$, that give rise to the same density $n_0(r)$. The associated Hamiltonians $\hat{H}_1$ and $\hat{H}_2$, will therefore have different groundstate wavefunctions ψ_1 and ψ_2, that each yield $n_0(r)$. Using the variational principle together with yields,

$$E_1^0 < \langle \psi_2 \mid \hat{H} \mid \psi_2 \rangle + \langle \psi_2 \mid \hat{H}_1 - \hat{H}_2 \mid \psi_2 \rangle = E_2^0 + \int n_0(r)[V_{ext,1}(r) - V_{ext,2}(r)]dr \tag{2.39}$$

where F_1^0 and F_2^0 are the groundstate energies of $\hat{H}_1$ and $\hat{H}_2$ respectively. It is at this point that the Hohenberg-Kohn theorems, and therefore DFT, apply rigorously to the groundstate only. An equivalent expression holds when the subscripts are interchanged. Therefore adding the interchanged inequality leads to the result:

$$E_1^0 + E_2^0 \; < \; E_2^0 + E_1^0 \tag{2.40}$$

which is a contradiction, and as a result the groundstate density uniquely determines the external potential , to within an additive constant. Stated simply, the electrons determine the positions of the nuclei in a system, and also all groundstate electronic properties, because as mentioned earlier, $V_{ext}(r)$ and N completely define $\hat{H}$.

2.7.2 Theorem 2

Obtaining the groundstate energy can be done in a variety of ways: The exact groundstate density is the density that has the least amount of total energy [32]. The proof of the second theorem is also straightforward: as just shown, $n(r)$ determines $V_{ext}(r)$, and determine $\hat{H}$ and therefore ψ. This ultimately means ψ is a functional of $n(r)$, and so the expectation value of $\hat{F}$ is also a functional of $n(r)$, i.e.

$$F[n(r)] = \langle \psi \mid \hat{H} \mid \psi \rangle \tag{2.41}$$

A density that is the ground-state of some external potential is known as ν-representable. Following from this, a ν-representable energy functional $E_v[n(r)]$ can be defined in which the external potential $\nu(r)$ is;

$$E_v[n'(r)] = \int n'(r)\nu_{ext}(r)dr + F[n'(r)] \tag{2.42}$$

unrelated to another density $n'(r)$.

And the variational principle asserts,

$$\langle \psi^{'} \mid \hat{F} \mid \psi^{'} \rangle + \langle \psi^{'} \mid \hat{V_{ext}} \mid \psi^{'} \rangle \; > \; \langle \psi^{'} \mid \hat{F} \mid \psi^{'} \rangle + \langle \psi \mid \hat{V_{ext}} \mid \psi \rangle \tag{2.43}$$

$$\int n^{'}(r)\nu_{ext}dr + F[n^{'}(r)] \; > \; n(r)v_{ext}(r)dr + F[n(r)]dr \tag{2.44}$$

where the wavefunction ψ is associated with the correct ground state. This leads to, and so the variational principle of the second Hohenberg-Kohn theorem is obtained. However, despite the fact that the Hohenberg-Kohn theorems are exceedingly powerful, they do not provide a practical method of determining the ground-state density of a system. Just over a year after Hohenberg and Kohn's foundational DFT publication, Kohn and Sham established a straightforward method for carrying out DFT

computations that keeps the exact essence of DFT [33].

$$E_v[n^{'}(r)] > E_v[n(r)] \tag{2.45}$$

Hohenberg-theory Kohn's demonstrates that the ground state density can be used to compute the system's attributes, but it does not provide a mechanism to find the density. The Kohn-Sham equations propose a way to get there. Let us begin by examining the ground state energy, which is represented as a function of charge density.

$$\begin{aligned} E[\rho(r)] &= T[\rho(r)] + \int \rho(r)\nu(r)dr + E_{ee}[\rho(r)] \\ &= \frac{1}{2}\frac{\rho(r)\rho(r)^{'}}{\mid r - (r)^{'} \mid}drdr^{'} + E_{xc}[\rho(r)] \end{aligned} \tag{2.46}$$

Three terms are used to describe the movement of electrons: kinetic energy, interaction with the external potential, and ion-electron interaction. The electron-electron electrostatic interaction is represented by the first term on the right hand side of the equation, while the non-classical exchange-correlation energy is represented by the second term [34].

2.8 Kohn-Sham equation

The KohnSham equations are named after Walter Kohn and Lu Jeu Sham, who introduced the concept at the University of California, San Diego, in 1965. The Kohn-Sham equations are a set of eigenvalue equations within DFT. Kohn-Sham theory in particular has laid the groundwork for the application of DFT in computational chemistry. This theory is based on the idea that electron density is a perfect predictor of ground state electrical energy. Kohn and Sham derived a set of single particle by reintroducing wavefunctions ψ_i with where n is the number of electrons. The kinetic energy is given by,

$$\int \psi_i^*(r)\psi_j(r)dr = \delta_{ij} \tag{2.47}$$

$$\rho(r) = \sum_{i=1}^{M} \psi_i^*(r)\psi_i(r) \tag{2.48}$$

$$T[\rho(r)] = -\frac{\hbar^2}{2m}\sum_{i=1}^{n}\langle\psi_i \mid \bigtriangledown^2 \mid \psi_i\rangle \tag{2.49}$$

If the wavefunctions are required to be orthonormal, i.e. then we can define a functional of the wavefunctions,

$$\Omega[\psi_i] = E[\rho(r)] - \sum_i \sum_j \xi_{ij} \int \psi_i^*(r)\psi_j^*(r)dr \tag{2.50}$$

where ξ_{ij} are Lagrange multipliers to ensure the wavefunctions are orthonormal. Minimization of $\Omega[\psi_i]$ with respect to $\psi^*(r)$ gives the Kohn-Sham equations

$$[-\frac{\hbar^2}{2m} \bigtriangledown^2 + \nu_{eff}(r)] = \xi_i\psi_i(r) \tag{2.51}$$

where ν_{xc} is the exchange-correlation potential given by,

$$\nu_{xc}(r) = \frac{\partial E_{xc}}{\partial \rho(r)} \tag{2.52}$$

However, a nonlocal potential exists in the HF equations, which is in contradiction to this.

2.9 Exchange-correlation functional

LDA is a single local exchange-correlation functional supported by CASTEP; GGA is a set of three gradient-corrected exchange-correlation functionals; and a set of nonlocal functionals for self-consistent total energy calculations are also supported. When it comes to CASTEP, CA-PZ is the sole LDA function available [35]. In comparison to LDA functionals, the GGA functionals offer a more comprehensive picture of the electrical subsystem. By overbinding atoms, the LDA description tends to overstate bond lengths and cell volume by a few percent, resulting in an overestimation of the bulk modulus. While correcting this problem, GGA can lead

to bonds that are slightly longer than they should be PBE is the default correlation function for exchange rates [36]. Even though it may be used in bulk calculations, it is recommended for studies of molecules interacting with metal surfaces. Nonlocal functional RPBE, a refined version of the PBE functional, is designed to better describe metallic surfaces. GGA lattice constants, crystal structures, and metal surface energies have all been significantly improved over the PBE GGA. Improved structural and energy properties for densely packed solids and their surfaces have been achieved with the help of a new functional called PBEsol. CASTEP is capable of handling functionals that are dependent on the kinetic energy density in addition to GGA functionals, which are dependent on the local density and its gradient, among other things. As opposed to pure GGA functionals, meta-GGA functionals are believed to be more precise and the cost of performing such computations is much less expensive than the cost of performing nonlocal functionals. As a result of the generalized Kohn-Sham approach , nonlocal exchange-correlation functionals are produced, which are expected to improve the description of band gaps in insulators and semiconductors as compared to LDA or GGA computations [37]. This increased accuracy comes at the expense of longer calculations that take more time to complete. Several approximations for nonlocal exchange-correlation functionals are available: (i) HF, (ii) HF-LDA, (iii) sX, (iv) sX-LDA, (v) PBE, (vi) B3LYP, (vii) HSE03, (viii) HSE06, (ix) PBE0, (x) B3LYP, and (xi) HSE06 are the functionals most commonly used for testing against alternative HF methods for solids implementations. For the most part, DFT does not have a good handle on the functionals for exchange and correlation. Approximations, on the other hand, allow for the precise determination of some physical quantities. One of the simplest approximations is the LDA, where the functional depends simply on density at a given point.

$$E_{XC}^{LDA}[n] = \int \epsilon_{XC}(n)n(r)d^3r \tag{2.53}$$

Local spin density approximation is a simple extension of the LDA to add electron spin:

$$E_{XC}^{LDA}[n_\uparrow, n_\downarrow] = \int \epsilon_{XC}(n_\uparrow, n_\downarrow)n(r)d^3r \tag{2.54}$$

It is common in LDA for the exchange correlation energy to be divided into two components: $XC = X + C$. The Dirac (or Slater) exchange takes the form $X\ n^{1/3}$ for the exchange portion. Correlation can, however, take many different mathematical shapes. According to the results of jellium quantum Monte Carlo simulations, the correlation energy density $nC(m, m)$ may be accurately calculated. In addition, a simple first-principles correlation functional has recently been presented. As a result, both forms of Monte Carlo simulation are equally accurate [38]. The Kohn-Sham density-functional scheme's exchange-correlation potential is the difference between the Fermi potential (an effective potential appearing in the one-electron Schrdinger equation for the square root of the electron density) and the Pauli potential. The Fermi potential can be estimated or modeled directly from the system's interacting two-electron reduced density matrix. The unified treatment of these three potentials provides a practical method for obtaining accurate functional derivatives of the exchange-correlation, Pauli kinetic, and Levy-Perdew-Sahni energy functionals without having to deal with the functional differentiation and numerical difficulties associated with other construction techniques. We create exchange-correlation functionals by fitting the functional form to higher-level theory data (for example, wave function method results for gas phase chemistry) and experimental benchmark data for bulk cohesive and elastic characteristics, as well as surface chemistry.

Using the LDA, one assumes that the density is the same everywhere. As a result, the LDA tends to overestimate the correlation energy while underestimating the exchange energy. Due to the exchange and correlation parts, the mistakes are likely to compensate for each other. Because of the non-homogeneity of the genuine electron density, it is usual to counteract this tendency by extending the gradient of the density. This enables for adjustments based on density variations away from the coordinate. Generalized gradient approximations (GGA) are a type of expansion that takes the following form:

$$E_{XC}^{GGA}[n_\uparrow, n_\downarrow] = \int \epsilon_{XC}(n_\uparrow, n_\downarrow) n(r) d^3r \tag{2.55}$$

The latter (GGA) has shown excellent results in terms of molecular geometries and

ground-state energies. As a natural progression from the GGA functionals, the new meta-GGA functionals have the potential to be even more precise than the GGA functionals themselves.

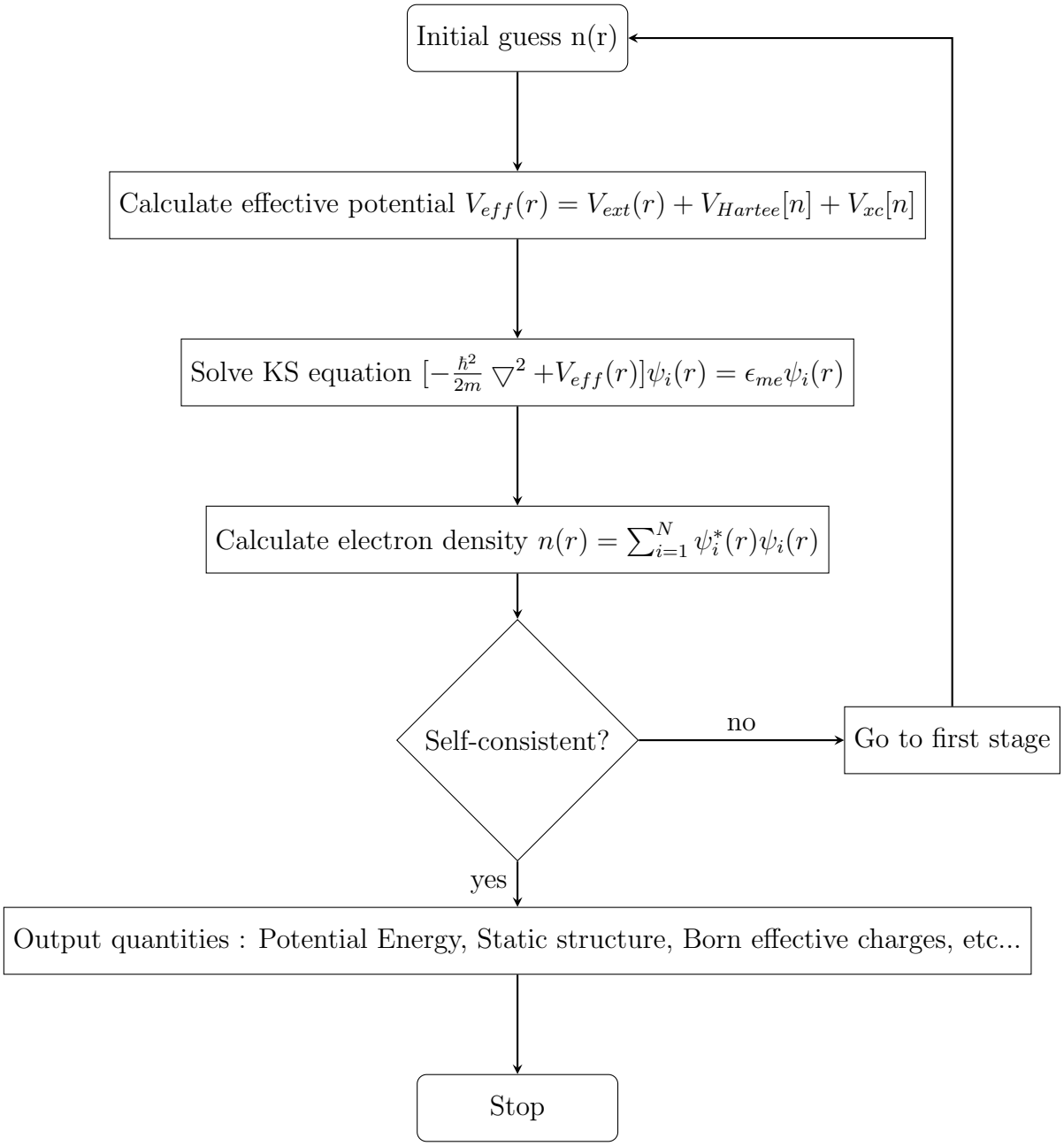

The Laplacian (the second derivative of the electron density) is included in the original Meta-GGA DFT functional, whereas GGA only includes the density and its first derivative. TPSS and Minnesota Functionals are examples of functionals of this type [39]. The density, gradient, and Laplacian (second derivative) of the density all play a role in the expansion of these functionals. A component of the actual

HF exchange energy can alleviate difficulties in expressing the energy's exchange portion. The term "hybrid functionals" is used to describe these kinds of functions.

Chapter 3

Electronic, magnetic and optical properties of LaP

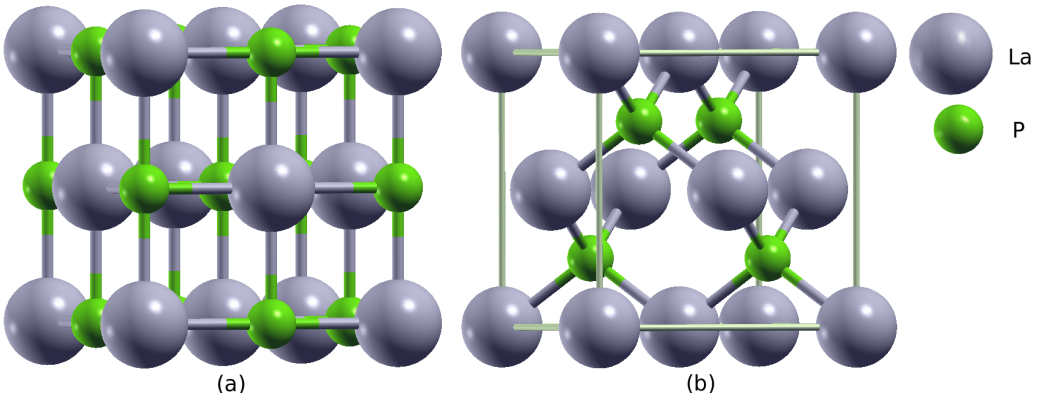

Figure 3.1: Crystal structure of LaP (a) rock-salt type, (b) zinc-blende type obtained with XCrySDen

Lanthanum phosphide is an inorganic compound of lanthanum and phosphorus with the chemical formula LaP. Other names for this chemical include Phosphanylidynelanthanum and Phosphanylidynelanthanum. It has a molar mass of 169.88 and appear like a black crystal. It interacts with water and has a density of 5.2 g/cm^3. Its crystalline structure is made up of cubic forms. The chemical forms cubic black crystals with cell parameters of a = 0.601 nm and a number of formulas per unit cell of Z = 4. The crystals are highly unstable and decompose into the open air.

Table 3.1: Equilibrium energy and lattice constant of LaP for NM and FM calculation

Compound	Structure	Calculation	Lattice constant (Å)	Equilibrium energy (Ry)
LaP	RS	NM	6.0590	-17679.76
		FM	6.0580	-17679.76
	ZB	NM	6.6291	-17679.69
		FM	6.6294	-17679.69

3.1 Computational method

By first-principles resolving the Kohn-Sham equation, we analyzed the electronic, magnetic, and optical characteristics of LaP within a self-consistent framework. We employed PBE (Perdew Burke Ernzerhof) potential for structural optimization. Electronic and optical computations were carried out using the WIEN2k code's modified Becke-Jonhson potential (mBJ) in order to acquire more precise findings. The self-consistent full potential linearized augmented plane wave (FP-LAPW) approach was used for all computations. This approach divides the unit cell into two regions: the interstitial area and the non-overlapping (muffin-tin) spheres. Within the muffin-tin sphere (MT), the basic functions are extended into spherical harmonic functions, and in the interstitial area, Fourier series are generated. Both the La and P atoms' MT sphere radii were chosen to be 2.3 a.u.

We performed volume optimization calculations for each potential in order to acquire the optimal theoretical lattice parameters that provide the lowest energy value. This computation was performed for both ferromagnetic and non-magnetic types. We employed the Murnaghan equation of state for this purpose. We can determine which structure of LaP is the most stable by displaying volume vs energy. This stable structure serves as the foundation for calculations of future electronic and magnetic properties.

Rare-earth LaP studies are typically done in the RS structure with space group Fm-3m 225, with La atoms at (0, 0, 0) and P atoms at $(\frac{1}{2}, \frac{1}{2}, \frac{1}{2})$. This is the most common structure used in these studies. P occupies site $(\frac{1}{4}, \frac{1}{4}, \frac{1}{4})$ in ZB structure (space group 216), while La atom occupies (0, 0, 0) site. An equilibrium lattice constant of 6.294

$\mathring{A}$ was determined for LaP in the ferromagnetic state. The calculation were done with $R_{MT}{*}k_{max} = 8.5$, to attain energy eigen value convergence. The smallest radius of muffin-tin (MT) spheres is R_{MT} and the maximum value of the wave vector is k_{max}. The irreducible Brillouin zone (BZ) of ZB structure has been decomposed into a matrix of Monkhorst-Pack K-points. The iteration procedure is continued with total energy and charge convergence to 0.00001Ry and 0.0001e respectively. The largest possible vector in charge density Fourier expansion (G_{max}) has a magnitude of twelve. There was a cutoff energy of -6 Ry that separated the valence electrons from the core electrons. There are $10 \times 10 \times 10$ K-points in the BZ that we used for energy calculations, which is 1000 K-points in the total zone. It is required to use denser K-meshes to calculate density of states and transport properties, therefore we used 10000 K-points in the entire BZ. For magnetic and non-magnetic calculations of RS type structure, the energy vs volume graph overlap with one another as there values are closely related to each other. The same results also appear for ZB type structure while we calcule energy vs volume for it's magnetic and non-magnetic phases.

3.2 Electronic and Magnetic Properties

In this section, we have examined the electronic characteristics of LaP by calculating the energy bandstructure, DOS, and charge distribution. We computed both PDOS and DOS in order to better understand how these systems are bonded. This bandgap significance states that the LaP compound is a semiconductor because of the substantial bandgap between the conduction and valence bands.

3.2.1 Band structure for magnetic calculation

Analysis of major electronic features (band structure and DOS) is essential for gaining a strong understanding of optical functions. Figure 3.2 depicts the analyzed band configurations of LaP. The Fermi level (E_F) is shown at zero on the photon energy scale, which ranges from -5 eV to + 5 eV for the sample. According to semiconductive theory, the material band structure near to the E_F is a highly important

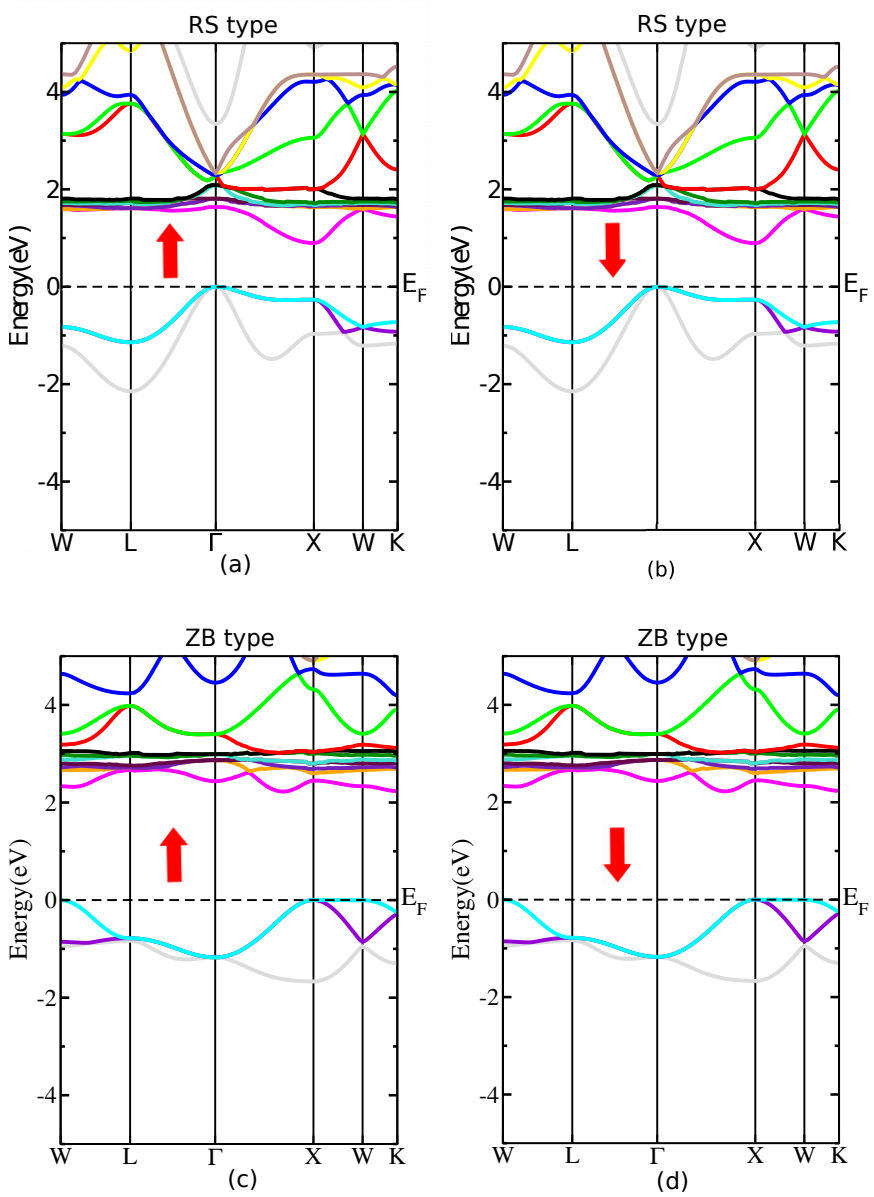

Figure 3.2: Band structure of LaP in mBJ for both spin channel of (a,b) rock-salt type, (c,d) zinc-blende type structure obtained with XCrySDen

criterion for learning about the material's physical nature. As a result, we've shown the band structure arrangement near the Fermi level. The calculation is done by defining highly symmetric points on the edge of the BZ with sampling path of W-L-Γ-X-W-K. We observed energy-band structures for the equilibrium geometry of LaP along higher symmetry directions in the BZ. Figure 3.2 shows that for the both spin channels of the RS type structure with an average energy band gap of 0.896 eV, the valence band maximum (VBM) is situated at the high symmetry point Γ and the conduction band minimum (CBM) is positioned at the X in the BZ. The

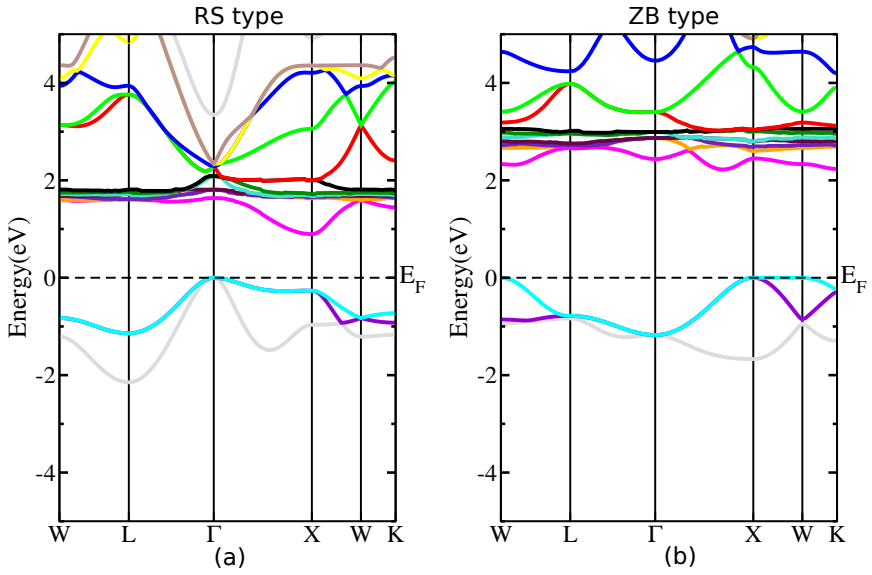

Figure 3.3: Band structure of LaP in mBJ for (a) rock-salt type, (b) zinc-blende type structure obtained with XCrySDen

VBM is positioned at the high symmetry point W and the CBM is located at the K in the BZ with an indirect band gap of 2.259 eV for the both spin channels of the ZB type structure.

3.2.2 Band structure for non-magnetic calculation

In the RS type structure, the VBM is located at the high symmetry point Γ and the CBM is located at the K in the BZ with an indirect band gap of 0.896 eV, whereas in the ZB type structure, the VBM is located at the W and the CBM is located at the K in the BZ with an indirect band gap of 2.258 eV which is shown in Figure 3.3. For all cases, f-La contributes the most in the conduction band, whereas p-P contributes the most in the valence band.

As illustrated in Figures 3.4 and 3.5, the electronic properties of LaP are clearly found by using the mBJ to compute the total and partial DOS inside the magnetic phase chosen for spin-up and spin-down channel. The p orbitals of P provide a significant contribution to the electronic states at the E_F in the valence band of LaP in both the spin up and spin down channels. In the same energy ranges where triply degenerate $d - t_{2g}$ (d_{xy}, d_{yz}, d_{zx}) states contribute most, a little contribution owing

Table 3.2: Energy bandgap (in eV) of LaP in PBE and mBJ approaches

Compound	Lattice type	Method	Calculation	Band gap (eV)	
				Spin up	Spin down
LaP	RS	PBE	NM	0.346	
			FM	0	0
		mBJ	NM	0.896	
			FM	0.897	0.895
	ZB	PBE	NM	1.528	
			FM	1.531	1.530
		mBJ	NM	2.258	
			FM	2.259	2.259

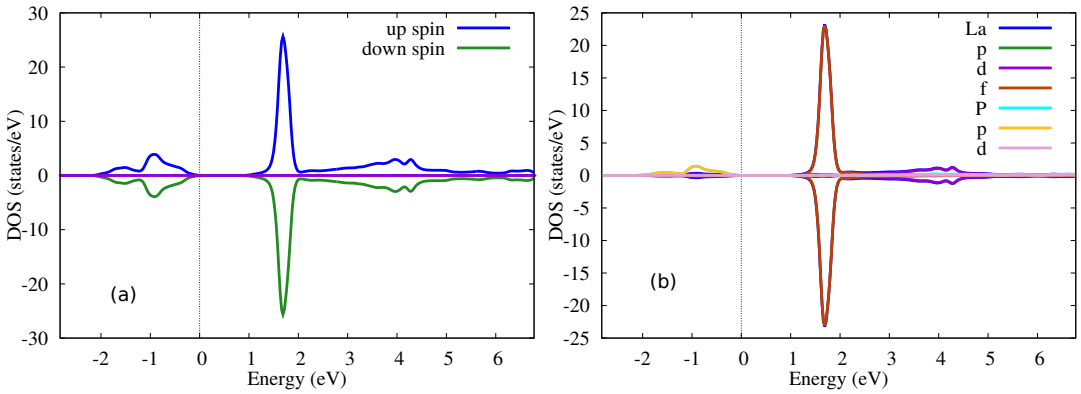

Figure 3.4: Total DOS and PDOS of LaP with its orbital contribution in rock-salt for both spin channel

to d-La orbitals upon hybridization is also expected. According to the results of the mBJ method, the contribution of f-La states to the conduction band is dominating in the energy range of 0.9 eV to 2 eV, whereas the contribution of p-P states to the electronic band formation is dominant from -2 eV to energy 0 eV, for RS type structure as shown in Figure 3.4. The contributions of the orbitals to the total DOS for the valence and conduction bands of the ZB type structure are shown in Figure 3.5. Compared to an RS type structure, there is a significant bandgap of 2.259 eV between the valence and conduction bands. While the p orbital's contribution to the conduction band is minimal, it is larger in the valence band. In the conduction band for 2.8 eV, f-La locates the greatest peak.

Each iteration of the self-consistent cycle yields spin-up and spin-down densities, and

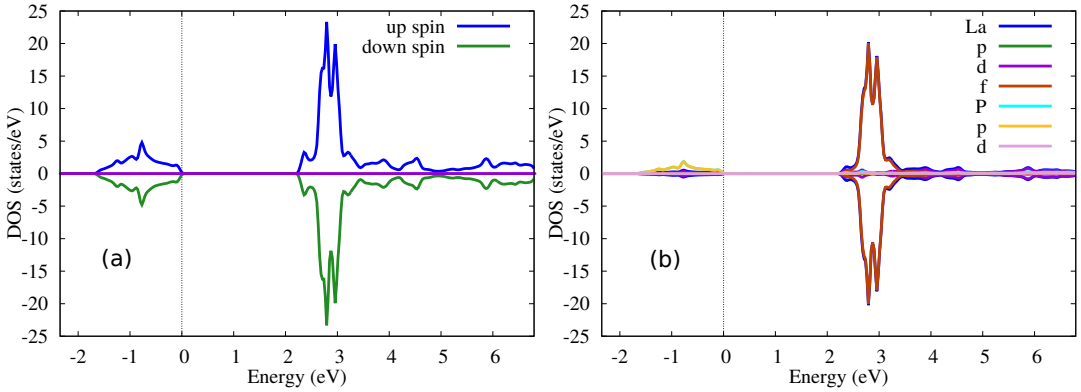

Figure 3.5: Total DOS and PDOS of LaP with its orbital contribution in zinc-blende for both spin channel

the difference or spin polarization, which is defined as the spin magnetic moment, is determined. The employed convergence criteria of 10^{-4} on electron charge density guarantees that the resulting magnetic moments are optimized with the same precision. We estimated individual atom magnetic moments, which are displayed in Table 3.3, where we can also observe the contribution of each atoms in LaP. P orbital has a positive integer in both PBE and mBJ potentials, while La has a negative integer. LaP exhibits a zero magnetic moment, revealing its diamagnetic properties. We utilized the same (R_{MT}) for all atoms in our computation. According to the Slater-Pauling rule, the total magnetic moment is $M_t = Z_t - 8$. Using the Slater-Pauling rule, we find that LaP have magnetic moments of 0 μB.

Table 3.3: Total spin magnetic moment of LaP in GGA and mBJ approaches

Compound	Structure	Individual magnetic moment (μB)		
		Site	GGA	mBJ
LaP	ZB	Intersititial	-0.00069	-0.00054
		La	0.00020	-0.00013
		P	0.00056	0.00067
		Total	0.00007	0.00000

3.3 Optical Properties

The optical properties of a material are important to know how the materials respond to the electromagnetic radiations. Examining LaP's optical characteristics can yield a slew of new optoelectronic uses. As LaP's properties are so complex, we calculated its dielectric function and absorption coefficient as well as electron energy loss, reflection, refraction and optical conductivity.

3.3.1 Dielectric Function

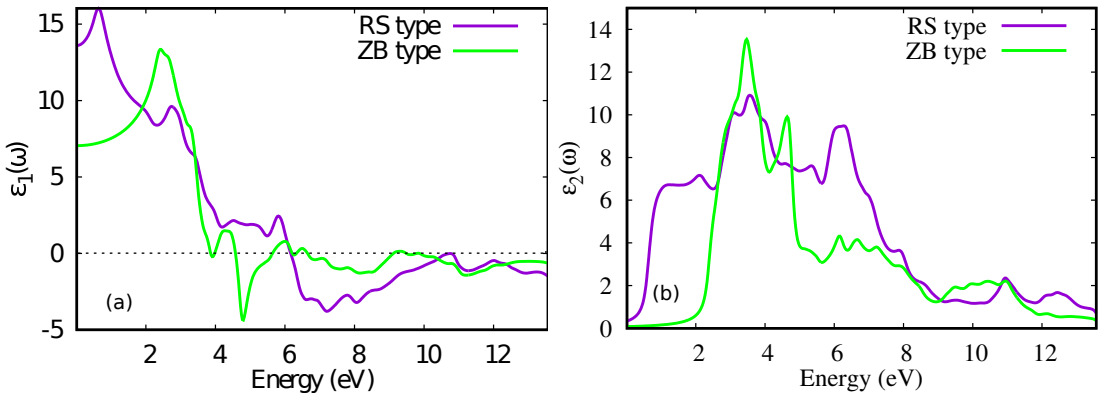

Figure 3.6: (a) Real part of dielectric function $\epsilon_1(\omega)$ and (b) Imaginary part of dielectric function $\epsilon_2(\omega)$ as a function of energy for LaP with mBJLDA

Complex dielectric function is one of the best strategies to investigate the optical properties of LaP. The dielectric function:

$$\epsilon(\omega) = \epsilon_1(\omega) + i\epsilon_2(\omega) \tag{3.1}$$

where $\epsilon_1(\omega)$ and $\epsilon_2(\omega)$ that are real and imaginary parts of the complex dielectric function respectively . This dielectric functions can be used to describe the linear response of the systems to electromagnetic radiations. The real $\epsilon_1(\omega)$ and imaginary part $\epsilon_2(\omega)$ of dielectric constant as a function of energy were plotted in Figure 3.6 where energy plotted in the x-direction, and real and imaginary dielectric tensor plotted in the y-direction.

As seen in Figure 3.6(a), the static value of the real part of dielectric constant depending on and $\epsilon_1^{xx}(0)$ and $\epsilon_2^{zz}(0)$ are found at 13.7 and 7.1 eV respectively. Here

maximum peaks are for 0.7 eV and 2.6 eV respectively and the minimum peaks are 4.8 eV and 7.2 eV for RS and ZB type of structure. The imaginary part of the dielectric function shows that the absorption starts before 0.1 eV. Strong optical transitions are caused by the greatest peak of the imaginary component of the dielectric constant, which is positioned at approximately 3.1 eV and 3.2 eV for RS type and ZB type structure respectively energy ranges for LaP in the energy spectrum. This dispersive conductivity of RS type LaP structure specializes extremely good in infrared region wherein ZB type structure specializes extremely good in the visible range. Thus it works effectively through the ultraviolet region.

3.3.2 Absorption Coefficient

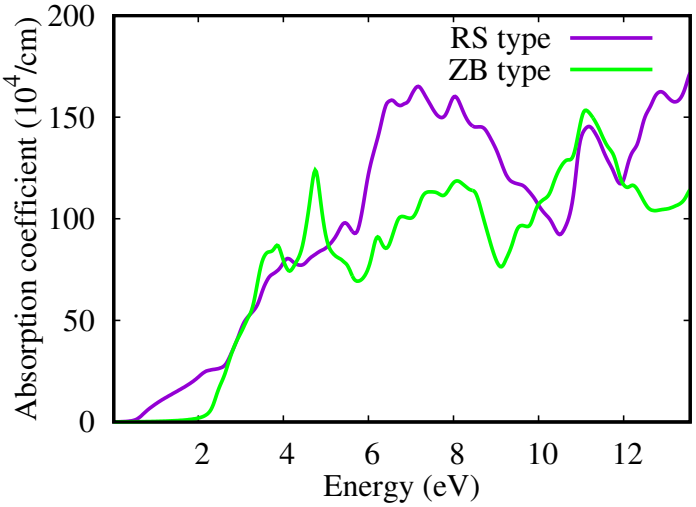

Figure 3.7: Calculated absorption coefficient as a function of energy for LaP with mBJLDA

It is essential to determine how far a material light of a particular wavelength can penetrate before absorption. It is provided as follows,

$$\alpha(\omega)_j = \frac{2\omega}{c}[-Re(\epsilon c\omega)j + \frac{|\epsilon(\omega)_j|}{2}]^{1/2} \tag{3.2}$$

We have calculated the absorption coefficient of LaP, which has been plotted in Figure 3.7. The horizontal line shows energy (eV), and the vertical line indicates the absorption coefficient (10^4/cm). We can see, the value of the absorption coefficient

promptly increases when the incident energy becomes higher. The maximum value of RS type and ZB type structure is 6.7 eV and 11 eV respectively, in the ultraviolet region. It shows both types of structure works inadequately in infrared region. This analysis result indicates that the frequency area of 6 eV to 11 eV is the strongest absorption zone for LaP. The value of absorption coefficient rapidly increases when the incident photon energy became higher region and this is a typical characteristics of a semiconductors.

3.3.3 Electron Energy Loss

Energy loss function is the energy lost by a fast-moving electron as it travel through a substance. It's a very significant phase since it offers information about the sample or material's structure and chemical composition. From the dielectric function, the electronic energy loss function of material can be furthur to describe the energy loss when electrons pass through a uniform dielectric. Electron loss (in arbitrarily measured units) vs. Energy (eV) is shown graphically in Figure 3.8.

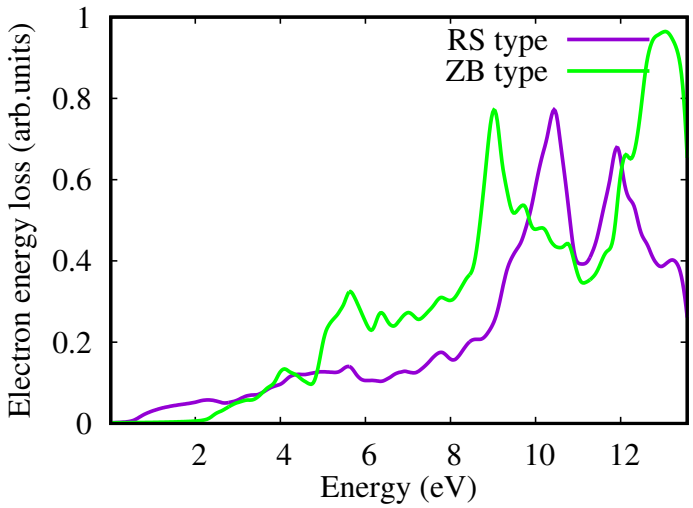

Figure 3.8: Calculated electron energy loss as a function of energy for LaP with mBJLDA

Both ZB and RS structures have their largest peaks in the ultraviolet, and their infrared performance is woefully lacking. This indicates that electrons in ZB structures don't lose energy in the infrared, while they do lose energy in the same region in RS structures.

3.3.4 Optical Reflectivity

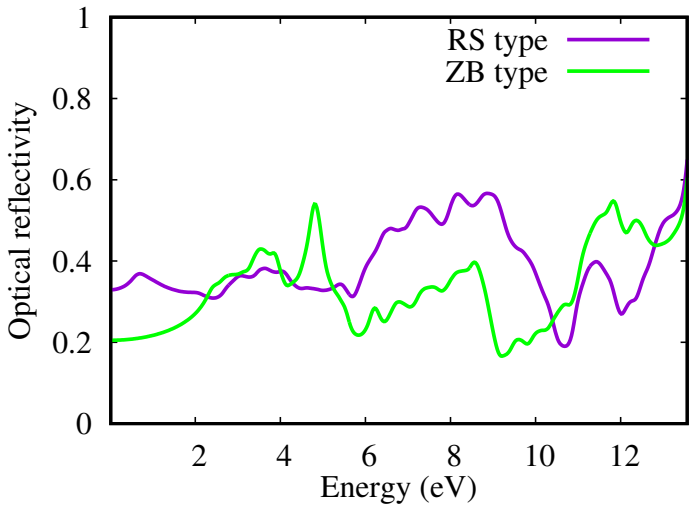

Figure 3.9: Calculated optical reflectivity as a function of energy for LaP with mBJLDA

Material reflectivity is important in determining how much light a material can reflect in relation to the amount of light it is exposed. Anti-reflective coatings are applied to a variety of materials to reduce the amount of light that is reflected. Figure 3.9 shows the relationship between optical reflectivity and energy in the infrared, visible, and ultraviolet ranges, with slightly higher peaks in the UV region. In the UV range, it appears that reflection is most effective. The lower reflectivity of LaP reveals that it is optical transparent in the photon energy range of 5 eV to 13.5 eV. Furthermore, there is a peak of reflectivity in the photon energy of 5 eV and 9 eV respectively for RS and ZB type structure.

3.3.5 Refractive Index

Another important physical quantity that describes a material's optical property is its refractive index (η). The refractive index of a material is very useful optical parameter to determine the propagation of light through the optical medium. The refractive index and the bandgap are inversely connected; as the refractive index rises, the bandgap falls, and vice versa. We have plotted refractive index vs Energy in Figure 3.10. Refractive index decreases steadily from the infrared to the ultraviolet, as depicted in the image. Refraction indices of RS and ZB types peak at 0.7 eV and

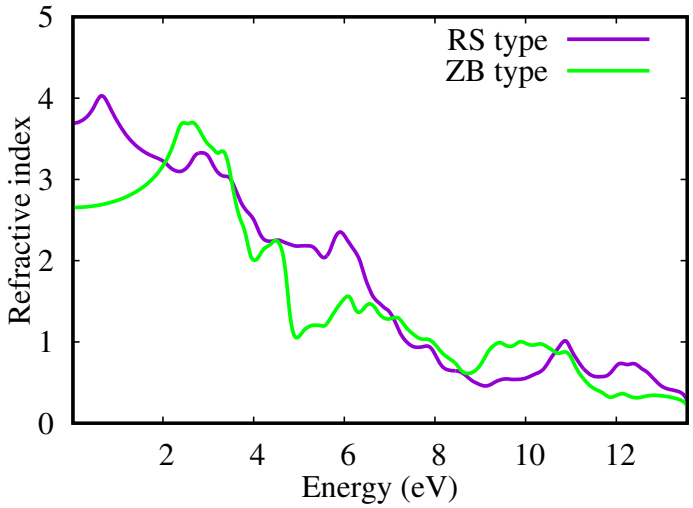

Figure 3.10: Calculated refractive index (η) as a function of energy for LaP with mB-JLDA

2.2 eV for these two materials, respectively.

3.3.6 Optical Conductivity

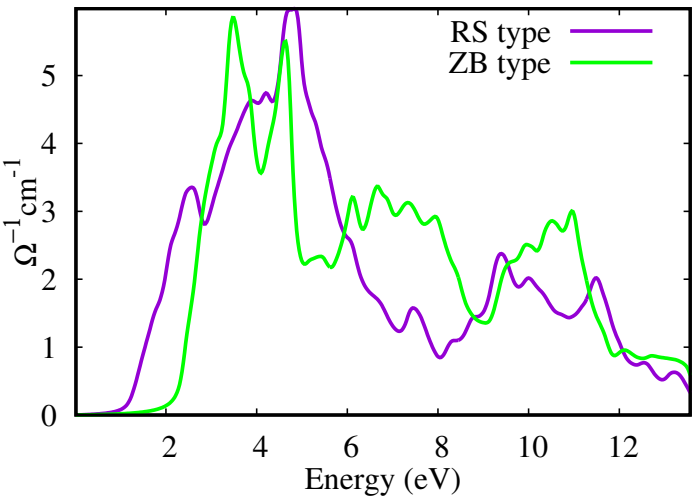

Figure 3.11: Calculated optical conductivity as a function of energy for LaP with mB-JLDA

The optical conductivity corresponds to the conduction of electrons produced when a photon of a certain frequency is incident upon a material. The optical conductivity along with it's energy is depicted in Figure 3.11. The optical conductivity for both type structures doesn't hold same type pattern. The threshold optical conductivity

differs for both of them. It's energy peak becomes high when it is in ultra violet region rather than infrared region. Thus we can conclude that both type of structure are optically conductive at a high proton energy range.

Chapter 4

Conclusion

We investigated the electronic, magnetic, and optical characteristics of LaP, a rare-earth phosphide, using first-principles simulations. For both ZB and RS structures, volume optimization reveals the surprising property that LaP performs significantly better in the FM computation. In accordance with the anticipated electronic band structure and DOS, FM calculation of ZB indicates better semiconducting behavior of LaP with indirect band gap of 2.259 eV. Optical characteristics such as dielectric constant, absorption coefficient, electron energy loss, optical reflectivity, refractive index, and optical conductivity are studied upto the energy range of 13.5 eV. According to the calculated electronic and optical characteristics of this compound, LaP is a promising choice for optoelectronic applications.

List of Abbreviations

DFT	:	Density Functional Theory
DOS	:	Density of States
GGA	:	Generalized Gradient Approximation
HK	:	Hohenberg-Kohn
KS	:	Kohn-Sham
LSDA	:	Local Spin Density Approximation
XC	:	Exchange Correlation
RS	:	Rock Salt
ZB	:	Zinc Blende
PBE	:	Perdew-Burke-Ernzerhof
mBJ	:	Modified Becke-Johnson
NM	:	Non Magnetic
FM	:	Ferromagnetic
GGA	:	Generalized Gradient Approximation
LDA	:	Local Density Approximation

Bibliography

[1] RD King-Smith, RJ Needs, V Heine, and MJ Hodgson. A first-principle calculation of the temperature dependence of the indirect band gap of silicon. *EPL (Europhysics Letters)*, 10:569, 1989.

[2] JWD Connolly and AR Williams. Density-functional theory applied to phase transformations in transition-metal alloys. *Physical Review B*, 27(8):5169, 1983.

[3] Nathan Argaman and Guy Makov. Density functional theory: An introduction. *American Journal of Physics*, 68:69–79, 2000.

[4] Chia-Min Lin, Wei-Chih Chen, and Cheng-Chien Chen. First-principles study of strain effect on the thermoelectric properties of lap and laas. *Physical Chemistry Chemical Physics*, 23:18189–18196, 2021.

[5] Ikram Un Nabi Lone, M Mohamed Sheik Sirajuddeen, SB Mohamed, and Saubia Khalid. A density functional calculations on electronic, magnetic, optical, mechanical and half-metallic properties in molybdenum based pnictogens in gga and gga+ u approach. *Materials Chemistry and Physics*, 260:124159, 2021.

[6] JJ Hernández Rosas, RE Ramírez Gutiérrez, A Escobedo-Morales, and Ernesto Chigo Anota. First principles calculations of the electronic and chemical properties of graphene, graphane, and graphene oxide. *Journal of molecular modeling*, 17:1133–1139, 2011.

[7] S Legvold. Rare earth metals and alloys. *Handbook of Ferromagnetic Materials*, 1:183–295, 1980.

[8] Sudhakar V Alapati, J Karl Johnson, and David S Sholl. Identification of destabilized metal hydrides for hydrogen storage using first principles calculations. *The Journal of Physical Chemistry B*, 110:8769–8776, 2006.

[9] Le Anh Thi, Man Minh Tan, Do Hoang Tung, Do Quang Tam, and Nguyen Minh Hoa. Cadmium selenium nanocrystal: first-principles insight into the structural, electronic, and optical properties. *Journal of the Korean Physical Society*, 80:910–913, 2022.

[10] Zein K Heiba, Mohamed Bakr Mohamed, Sameh Ahmed, et al. Optical and electronic correlation in mg-doped nano cadmium sulfide. *Optical and Quantum Electronics*, 53:1–17, 2021.

[11] Wei Ku, Tom Berlijn, Chi-Cheng Lee, et al. Unfolding first-principles band structures. *Physical review letters*, 104:216401, 2010.

[12] Pina Pitriana, Triati Dewi Kencana Wungu, Rahmat Hidayat, et al. The characteristics of band structures and crystal binding in all-inorganic perovskite apbbr3 studied by the first principle calculations using the density functional theory (dft) method. *Results in Physics*, 15:102592, 2019.

[13] Anubhav Jain, Shyue Ping Ong, Geoffroy Hautier, Wei Chen, William Davidson Richards, Stephen Dacek, Shreyas Cholia, Dan Gunter, David Skinner, Gerbrand Ceder, et al. Commentary: The materials project: A materials genome approach to accelerating materials innovation. *APL materials*, 1(1):011002, 2013.

[14] YO Ciftci, K Colakoglu, E Deligoz, and H Ozisik. The first-principles study on the lan. *Materials Chemistry and Physics*, 108:120–123, 2008.

[15] Masakatsu Suzuki, Takeshi Uenoyama, and Akira Yanase. First-principles calculations of effective-mass parameters of aln and gan. *Physical Review B*, 52:8132, 1995.

[16] S Laksari, A Chahed, N Abbouni, O Benhelal, and B Abbar. First-principles calculations of the structural, electronic and optical properties of cugas2 and aggas2. *Computational materials science*, 38:223–230, 2006.

[17] Ming-Hsien Lee, Po-Liang Liu, Yung-An Hong, Yen-Ting Chou, Jia-Yang Hong, and Yu-Jin Siao. Electronic band structures of ge1- xsnx semiconductors: A

first-principles density functional theory study. *Journal of Applied Physics*, 113:063517, 2013.

[18] Vladimir I Anisimov, Ferdi Aryasetiawan, and AI Lichtenstein. First-principles calculations of the electronic structure and spectra of strongly correlated systems: the lda+ u method. *Journal of Physics: Condensed Matter*, 9:767, 1997.

[19] Zhenhua Yang, Li Liu, Xianyou Wang, Shunyi Yang, and Xuping Su. Stability and electronic structure of the co–p compounds from first-principle calculations. *Journal of alloys and compounds*, 509:165–171, 2011.

[20] Guo-Xin Qian, Richard M Martin, and DJ Chadi. First-principles calculations of atomic and electronic structure of the gaas (110) surface. *Physical Review B*, 37:1303, 1988.

[21] Zhanhong Ma, Fengzhang Ren, Xiaoli Ming, Yongqiang Long, and Alex A Volinsky. Cu-doped zno electronic structure and optical properties studied by first-principles calculations and experiments. *Materials*, 12:196, 2019.

[22] Ming-Yang Liu, Yang Huang, Qing-Yuan Chen, Chao Cao, and Yao He. Unexpected electronic structure of the alloyed and doped arsenene sheets: First-principles calculations. *Scientific Reports*, 6:1–13, 2016.

[23] PH Jiang, HJ Liu, L Cheng, DD Fan, J Zhang, J Wei, JH Liang, and J Shi. Thermoelectric properties of γ-graphyne from first-principles calculations. *Carbon*, 113:108–113, 2017.

[24] Ikram Un Nabi Lone and M Mohamed Sheik Sirajuddeen. Half metallic ferromagnetism in gallium and zinc doped chromium phosphide: first principles calculations. *Materials Chemistry and Physics*, 203:65–72, 2018.

[25] Ikram Un Nabi Lone, M Mohamed Sheik Sirajuddeen, and S Rubab. A comparison study of the structural, electronic and magnetic properties in zinc-blende ptxcr1-xp and rhxcr1-xp (x= 0.125, 0.25), and half-heusler xcrp (x= pt, rh): First principles calculations. *Materials Chemistry and Physics*, 230:151–161, 2019.

[26] AF Kohan, Gerbrand Ceder, Dane Morgan, and Chris G Van de Walle. First-principles study of native point defects in zno. *Physical Review B*, 61(22):15019, 2000.

[27] Meng-Qiu Cai, Zhen Yin, and Ming-Sheng Zhang. First-principles study of optical properties of barium titanate. *Applied physics letters*, 83(14):2805–2807, 2003.

[28] Julian Schwinger. Thomas-fermi model: The leading correction. *Physical Review A*, 22(5):1827, 1980.

[29] Saadi Berri, D Maouche, N Bouarissa, and Y Medkour. First principles study of structural, electronic and optical properties of agsbs2. *Materials science in semiconductor processing*, 16(6):1439–1446, 2013.

[30] Claudia Ambrosch-Draxl, JA Majewski, P Vogl, and G Leising. First-principles studies of the structural and optical properties of crystalline poly (para-phenylene). *Physical review B*, 51:9668, 1995.

[31] R Asahi, Y Taga, W Mannstadt, and Arthur J Freeman. Electronic and optical properties of anatase tio 2. *Physical Review B*, 61:7459, 2000.

[32] DB Migas, VL Shaposhnikov, and VE Borisenko. Isostructural basi2, bage2 and srge2: electronic and optical properties. *physica status solidi (b)*, 244:2611–2618, 2007.

[33] Lijun Zhao, Xiaochao Zhang, Caimei Fan, Zhenhai Liang, and Peide Han. First-principles study on the structural, electronic and optical properties of biox (x= cl, br, i) crystals. *Physica B: Condensed Matter*, 407:3364–3370, 2012.

[34] F Elfatouaki, O Farkad, EA Ibnouelghazi, D Abouelaoualim, and A Outzourhit. Electronic and optical properties of csgex2m (x, m= br, cl, i) perovskites for solar cell applications: First-principles study using pbe and tb-mbj potentials. *Materials Science in Semiconductor Processing*, 143:106488, 2022.

[35] S Javad Mousavi. First–principle calculation of the electronic and optical properties of nanolayered zno polymorphs by pbe and mbj density functionals. *Journal of Optoelectronical Nanostructures*, 2:1–18, 2017.

[36] Saadi Berri, Miloud Ibrir, Djamel Maouche, and Mourad Attallah. First principles study of structural, electronic and magnetic properties of zrfetial, zrfetisi, zrfetige and zrnitial. *Journal of magnetism and magnetic materials*, 371:106–111, 2014.

[37] ZQ Lv, SH Sun, P Jiang, BZ Wang, and WT Fu. First-principles study on the structural stability, electronic and magnetic properties of fe2c. *Computational Materials Science*, 42:692–697, 2008.

[38] S Sarikurt, Y Kadioglu, F Ersan, E Vatansever, O Üzengi Aktürk, Y Yüksel, Ü Akıncı, and E Aktürk. Electronic and magnetic properties of monolayer α-rucl 3: a first-principles and monte carlo study. *Physical Chemistry Chemical Physics*, 20:997–1004, 2018.

[39] MAL Dantas, NF Frazão, David L Azevedo, and Jonas RF Lima. Electronic, magnetic and optical properties of penta-bn2 nanoribbons: A first principles study. *Computational Materials Science*, 190:110275, 2021.